Scientific
Research

Phase Transition Behavior of Nanocrystalline Al_2O_3 Powders

Balaraman Sathyaseelan[1], Iruson Baskaran[2], Kandasamy Sivakumar[3]

[1]Department of Physics, University College of Engineering Arni (A Constituent College of Anna University Chennai), Arni, India;
[2]Department of Physics, Arignar Anna Govt. Arts College, Cheyyar, India; [3]Department of Physics, Anna University Chennai, Chennai, India.
Email: bsseelan03@gmail.com, ibk1978@gmail.com, ksivakumar@annauniv.edu

ABSTRACT

Alumina (Al_2O_3) has been synthesized through combustion synthesis (CS) technique. The calcined products were characterized using X-ray diffractional analysis (XRD), scanning electron microscopy (SEM), transmission electron microscopy (TEM) and thermo-gravimetric analysis (TGA). TG-DTA results reveal the various stages involved in transition from γ-phase to α-Al_2O_3 phase. The first phase γ-Al_2O_3 was presented in the temperature range from 600˚C - 875˚C as deduced from the XRD patterns with cubic crystal structure. The second stage occurs in the temperature range from 900˚C - 1000˚C. In the final step, above 1000˚C, the aluminium oxide appears completely as α-Al_2O_3, showing high crystallinity. The particle sizes are closely related to γ- to α-Al_2O_3 phase transition.

Keywords: Nanocrystalline Al_2O_3; Phase Transitions; γ-Al_2O_3; α-Al_2O_3; Differential Scanning Calorimetry (DSC); Electron Microscopy (TEM and SEM)

1. Introduction

Alumina (Al_2O_3) has been employed for a wide range of applications, like electronic packaging, catalysts, sensors, etc. [1,2]. There are 15 distinct crystallographic phases, on which γ and α forms are used for wide range of applications due to their distinct properties. The high surface area of γ-Al_2O_3 makes it useful for catalyst related applications [3,4], where as the polycrystalline α-Al_2O_3 is extensively used for ceramic applications [5,6].

Numerous synthesis techniques have been followed to obtain nanosized Al_2O_3 products. Treatment phase transformations in Al_2O_3 nanocrystallites from γ to α phase is a crucial factor to the monitored. The various phases of Al_2O_3 undergo a variety of transitions until the most stable α structure (α-Al_2O_3) is formed at a high temperature [1,2]. It is well known from reports in literature that for obtaining dense nanocrystalline Al_2O_3 products, either the phase transformation from γ to α phase has to be arrested or nanocrystalline α-Al_2O_3 powders have to be used [7-9]. Different types of high molecular weight organic fuels have been successfully employed to synthesize materials with high specific surface areas. However, with the use of these fuels, an additional calcinations step

is needed to obtain crystalline materials, making the process very expensive [10]. The use of urea in direct synthesis procedure facilitated the formation of crystalline materials due to the generation of a temperature [11].

Generally, combustion synthesis is an excellent technique for preparing high temperature materials because of its low cost, high yield and the ability to achieve high purity and single or multi phase complex oxide powders in the as-synthesized state [12]. In this way the heat input needs only to reach an ignition temperature so that an exothermic, self-sustaining reaction takes place between precursors such as metal nitrates (oxidizers) and a carbonaceous fuel (reducer) [13]. In fact, this auto-ignition process along with the self-propagating high temperature synthesis (SHS) has emerged as safe, simple and most economic process, which yields high purity powders with excellent homogeneity and fine particle sizes in the case of composite materials. Furthermore, as this process does not require any further processes of washing, filtration, drying, calcinations, addition of any acid or base, it becomes very fast. Moreover, the combustion synthesis (CS) procedure has many advantages as compared to conventional synthesis procedures; CS process can be used to produce novel phases with unique properties in materials

as pure compounds can be easily produced because of the high thermal gradient and rapid cooling rate. Because of the gas evolution, large particles or agglomerates can be disintegrated during the process and the products formed are of high purity. The resulting product is very fine particulates of friable agglomerates that can be easily ground to obtain a much finer particle size.

In this perspective, this paper aims to study the phase transformation (γ- to α-Al$_2$O$_3$) behaviour of Al$_2$O$_3$ samples prepared by combustion synthesis technique and to evaluate their characteristic properties. The different phases formed were characterized by various techniques.

2. Experimental Details

Analytical grade Aluminium nitrate Al(NO$_3$)$_3$·6H$_2$O and urea [(NH$_2$)$_2$CO] without the addition of water in the molar ratio 1:2 were directly mixed. Aluminium nitrate being hygroscopic absorbs moisture from the air forming a transparent slurry mixture. After homogeneous mixing, the solutions were condensed on a hot plate and fired for 30 minutes in a muffle furnace at 500°C. The resultant powders were subsequently annealed in the range of 600°C - 1000°C for 2 h to obtain nanocrystalline Al$_2$O$_3$. Thermal behaviours of the samples were studied by thermogravimetry analyzer (Nietzsche STA 409C) and differential thermal analyzer (WCR-1C) in N$_2$ at the heating rate of 20°C/min up to 1000°C. The powders were characterized to determine the crystalline size, structure and morphology. The structure of the samples was analyzed using Powder X-ray diffraction (XRD) technique (Rich Siefert, Model 3000) using CuKα1 (λ = 1.5406 Å) radiation. Then using XRDA software programme the lattice parameters were determined and the average crystallite size was calculated with Debye-Scherrer formula. The Al$_2$O$_3$ particles were studied using transmission electron microscopy (TEM, JEM-1200EX, JEOL), the dilute suspension of the Al$_2$O$_3$ powders on the carbon-coated copper grids also dried in air. The surface features of the as prepared and annealed samples were observed by scanning electron microscope (SEM; Hitachi S-3000N).

3. Results and Discussion

3.1. Growth Process and Reaction Mechanism for Al$_2$O$_3$ Formation

The individual reactivity of Al(NO$_3$)$_3$ with respect to urea combustion reactions assumed to take place in the case of metal nitrate/fuel binary mixtures are represented by the Equation (1)

$$6Al(NO_3)_3 + 15CH_4N_2O \rightarrow 3Al_2O_3$$
$$+15CO_2 + 30H_2O + 24N_2 \qquad (1)$$
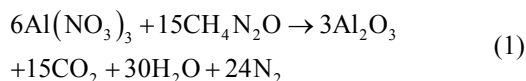
Al(NO$_3$)$_3$ the situation is quite opposite. The reaction

of Al(NO$_3$)$_3$ with urea (Equation (1)) was an intense and rather fast flaming combustion process. The formed Al$_2$O$_3$ nanoparticles were used for the further characterization.

3.2. Crystal Structure Determination

Figure 1(a) shows XRD pattern shows formation of mixed phases of Al$_2$O$_3$ along with the presence of non-stiochiometric as-synthesized precursor. Because of air as carrier gas, the deficiency of oxygen atoms may have lead to the formation of Al$_2$O$_3$ phase in the powder samples. The nonstiochiometric phase can be removed by heat treatment. **Table 1** gives the comparison of observed "d" values are in good agreement with standard "d" values and the diffraction peaks are indexed to the phase of Al$_2$O$_3$ [JCPDS No. 86-1410]. **Figures 1(b)-(d)** shows the XRD pattern of annealed γ-Al$_2$O$_3$ was revealed. It can be compared to transformation temperature the range from 600°C to 875°C, with low intensity which signified the transformation of mixed phase Al$_2$O$_3$ to γ-alumina is the only identified phase observed. Thermal treatment at 600°C to 875°C resulting with diffraction peaks at 2θ, 46.00° for (400) and 66.80° for (440) [JCPDS No. 29-0063] shows the sign of γ-Al$_2$O$_3$ phase. **Table 2** gives the comparison of observed "d" values are in good agreement with standard "d" values and the diffraction peaks are indexed to the phase of γ-Al$_2$O$_3$ [JCPDS No. 29-0063]. The degree of crystallinity was improved with increasing temperature. γ-Alumina was completely transformed to α-alumina at 900 to 1000°C α-alumina is

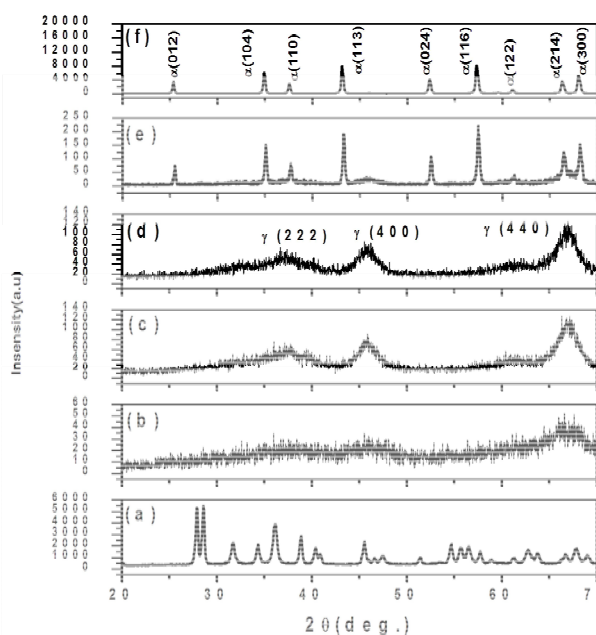**Figure 1. Powder XRD pattern of nanocrystalline Al$_2$O$_3$ sample, (a) as-prepared; (b) 600; (c) 850; (d) 875; (e) 900 and (f) 1000°C for 2 h.**

Table 1. Comparison of the observed "d" values with standard "d" values of as-prepared Al$_2$O$_3$ powder samples JCPDS No. 86-1410.

S.No	Observed d (Å)	Standard d (Å)	Plane (h k l)	Phase
1.	4.643	4.527	−2 0 1	Al$_2$O$_3$
2.	3.780	3.551	0 0 6	B-Al$_2$O$_3$
3.	2.820	2.820	−4 0 1	Al$_2$O$_3$
4.	2.611	2.567	−1 1 1	Al$_2$O$_3$
5.	2.484	2.447	1 1 1	Al$_2$O$_3$
6.	2.316	2.314	3 1 0	Al$_2$O$_3$
7.	2.232	2.250	−3 1 1	Al$_2$O$_3$
8.	1.947	1.953	−6 0 1	Al$_2$O$_3$
9.	1.914	1.909	6 0 0	Al$_2$O$_3$
10.	1.776	1.775	−6 0 2	Al$_2$O$_3$
11.	1.677	1.681	6 0 1	Al$_2$O$_3$
12.	1.649	1.651	−5 1 2	Al$_2$O$_3$
13.	1.627	1.621	5 1 1	Al$_2$O$_3$
14.	1.596	1.604	2 1 2	δ-Al$_2$O$_3$
15.	1.567	1.571	−1 1 3	Al$_2$O$_3$
16.	1.512	1.509	−6 0 3	Al$_2$O$_3$
17.	1.479	1.489	1 1 3	Al$_2$O$_3$
18.	1.458	1.455	0 2 0	Al$_2$O$_3$
19.	1.401	1.414	−8 0 2	Al$_2$O$_3$
20.	1.380	1.387	−7 1 2	Al$_2$O$_3$
21.	1.359	1.364	0 0 4	Al$_2$O$_3$

Table 2. Comparison of the observed "d" values with standard "d" values of annealed Al$_2$O$_3$ at 875˙C powder samples JCPDS No. 20-0063.

S.No	Observed d (Å)	Standard d (Å)	Plane (h k l)	Phase
1.	2.413	2.2800	(222)	Γ
2.	1.336	1.9800	(400)	Γ
3.	1.230	1.4000	(440)	Γ

the only present phase. The crystallite size of the α-Al$_2$O$_3$ it increases with increasing temperature. **Figures 1(e)-(f)**. shows XRD pattern of Al$_2$O$_3$ annealed above 900 to 1000˙C, matches well with that of α-Al$_2$O$_3$ with the diffraction peaks at 2θ values of, 25.37˙ for (012), 34.89˙ for (104), 37.50˙ for (110), 43.04˙ for (113), 52.58˙ for (024), 57.26˙ for (116) and 66.28˙ for (214) [JCPDS No. 42-1468]. No more appearance of other phases could be found in that temperature. **Table 3** gives the comparison

of observed "d" values are in good agreement with standard "d" values and the diffraction peaks are indexed to the phase of α-Al$_2$O$_3$ [JCPDS No. 29-0063]. The crystallite sizes of the nanocrystalline Al$_2$O$_3$ sample have been calculated using Scherrer formula [14]. The change in grain size is observed with broadening of the diffraction peaks. The mean crystallite size is calculated from the Scherrer formula listed in **Table 4**.

The particle size of γ-Al$_2$O$_3$ phase was increase corresponding to the respective annealing temperature. It was shown that γ-Al$_2$O$_3$ phase crystallite almost disappeared without growing up and α-Al$_2$O$_3$ phase crystallite rapidly grew up as transformation was completed. The α-Al$_2$O$_3$ phase crystallites could be obtained either through interface migration from α-Al$_2$O$_3$ nuclei or by coalescence among the α-Al$_2$O$_3$ nuclei and the two modes of formation result in the complete transition of γ-/α-Al$_2$O$_3$ phase. A high transformation temperature always results in the coarsening of particles and formation of hard agglomerates in the powder. Thus, a reduction in the γ-Al$_2$O$_3$ → α-Al$_2$O$_3$ transformation temperature is crucial for the processing of highly reactive ultra-fine α alumina powder. Strong peaks at 2θ, 43.04 for (113) and 57.26 for (116),

Table 3. Comparison of the observed "d" values with standard "d" values of annealed Al$_2$O$_3$ at 1000˙C powder samples JCPDS No. 42-1468.

S.No	Observed d (Å)	Standard d (Å)	Plane (h k l)	Phase
1.	3.602	3.4800	(012)	A
2.	2.438	2.5510	(104)	A
3.	2.407	2.3750	(110)	A
4.	2.355	2.0850	(113)	A
5.	1.293	1.7399	(024)	A
6.	1.268	1.6014	(116)	A
7.	1.251	1.5147	(122)	A
8.	1.231	1.4045	(214)	A
9.	1.226	1.3739	(300)	A

Table 4. Phase structure and crystallite size of the prepared Al$_2$O$_3$ annealed at different temperatures.

S. No.	Annealed temperature (˙C)	Crystallite size/nm	Phase structure
1.	As-prepared	-	-
2.	600	21	Γ
3.	850	36	Γ
4.	875	41	Γ
5.	900	70	A
6.	1000	75	A

are recognized, indicating α-Al$_2$O$_3$ phase according to the 42-1468 [JCPDS-PCPDFWIN, 2002].

3.3. Differential Thermalgravimetric Analysis

The thermal studies of these samples were carried out at the heating rate of 20˚C/min up to 1000˚C and the TG/DTA curves are given shown in **Figure 2**. From **Figure 2**, it is observed that the process of decomposition proceeds in two stages. The first step, ambient to endothermic peak at 195˚C is due to the dehydration of hydroxyl water of γ-AlOOH transformed to γ-Al$_2$O$_3$. In the temperature range from 150˚C to 340˚C, the 24.75% weight loss is much larger than the theoretical weight loss of the boehmite dehydration. It is known that the ultrafine boehmite powders have high special surface and easily adsorb water as hydration water which can exist stably to a certain temperature. It was reported [17] that pseudoboehmite typically contained excess water. The further weight loss at high temperature may result from the dehydration of the residual hydroxyl water in γ-Al$_2$O$_3$. The final step, from 340˚C to 630˚C, was due to the formation of Al$_2$O$_3$ with a weight loss of 11.556%. The net weight loss of the compound was found to be 36.30%. The DTA result of the as-prepared sample shows that the exothermic curves were associated with the corresponding weight loss in TGA curve of Al$_2$O$_3$ powder.

3.4. Differential Scanning Calorimetry

Figure 3 depicts the DSC trace of Al$_2$O$_3$ powders, in the temperature range of 100˚C to 550˚C at three different heating rates 10˚C, 15˚C and 20˚C/min. From the DSC trace, it is seen that at temperature below 260˚C, there are endothermic peaks due to the vaporization of physically bound absorbed water and the dehydration reaction of powders. It is important to note that these powders, irrespective of their urea-nitrate ratios, always show exothermal decomposition in their corresponding DSC
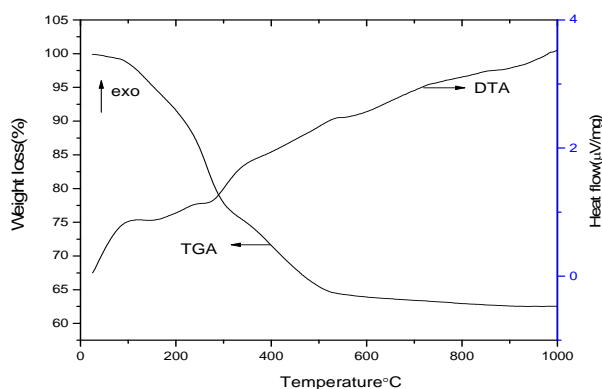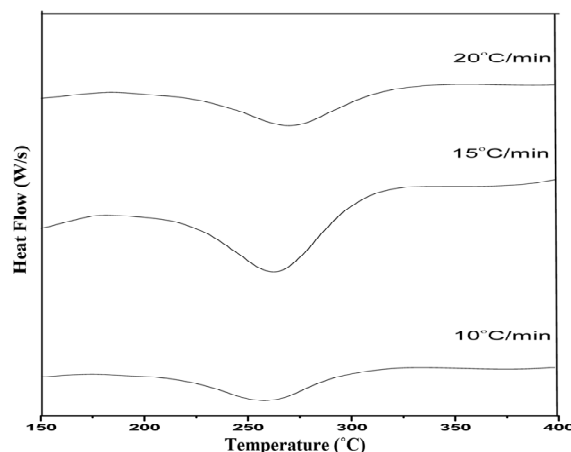

Figure 3. DSC pattern of as prepared Al$_2$O$_3$ powders at different heating rates (a) 10; (b) 15; and (c) 20˚C/min.

curves. It has been understood that such an exothermic reaction is a result of a thermally induced redox reaction, where urea acts as a reductant and nitrate as an oxidant [15-17]. The initial combustion temperature of the powder decreases, as the urea content in the powder increases in the fuel-lean condition. In the stoichiometric and fuel-rich conditions, the combustion temperature remains 260˚C with increase of γ phase of Al$_2$O$_3$ powders.

3.5. Scanning Electron Microscopy

The evolution of crystal morphology and grain size during the transformation was investigated by scanning electron microscopy (**Figures 4(a)-(f)**). The particles (500 nm) are composed of extremely small grain size with a size of 30 - 50 nm diameters, which is well consistent. The SEM micrographs of combustion samples that were annealed at 1000˚C for 2 h (**Figure 4(f)**) showed that all the grains were fairly regular with most of the grains smaller than 0.5 μm (500 nm) in size and some of the grains as small as 0.2 μm (200 nm). Another remarkable observation was the retention of ultra-fine grain size in this microstructure, as even most of the grains were less than 1μm in size, with a narrow size distribution.

3.6. Transmission Electron Microscopy

The TEM micrographs of the sample annealed at 875˚C for γ-Al$_2$O$_3$ is shown in **Figure 5(a)**. TEM micrographs reveal the nanocrystalline nature of the products. These results are in close agreement with the crystallite size estimated by X-ray line broadening for the same sample. **Figure 5(b)** shows the TEM image of α-Al$_2$O$_3$ annealed at 1000˚C for 2 h. Transformation of all pure Al$_2$O$_3$ into the single α phase was observed at temperature of 1000˚C, as indicated by **Figures 5(a)** and **(b)**. The sharp peaks of α phase indicate the relatively large grain sizes and well-defined long-range order in corundum. It can be

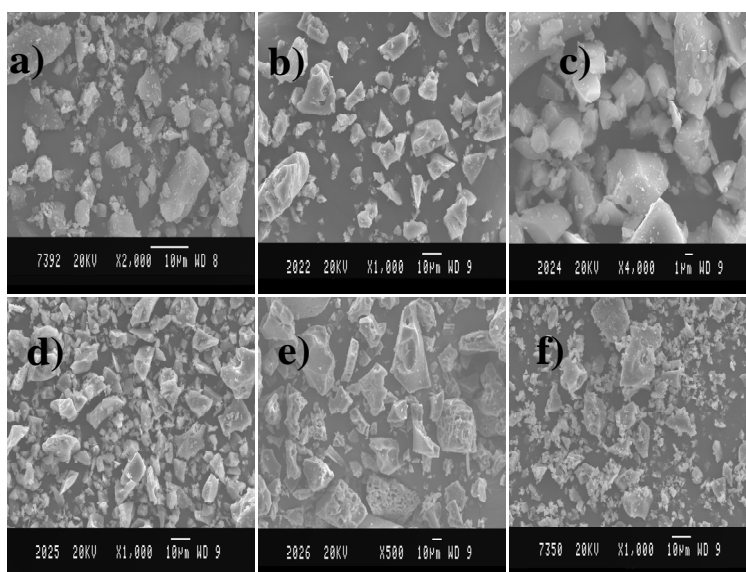**Figure 2. TGA/DTA analysis of the as prepared Al$_2$O$_3$ powders.**

Figure 4. SEM micrographs of nanocrystalline Al$_2$O$_3$ powders at different annealing condition: (a) as-prepared; (b) 600; (c) 850; (d) 875; (e) 900 and (f) 1000˙C for 2 h.
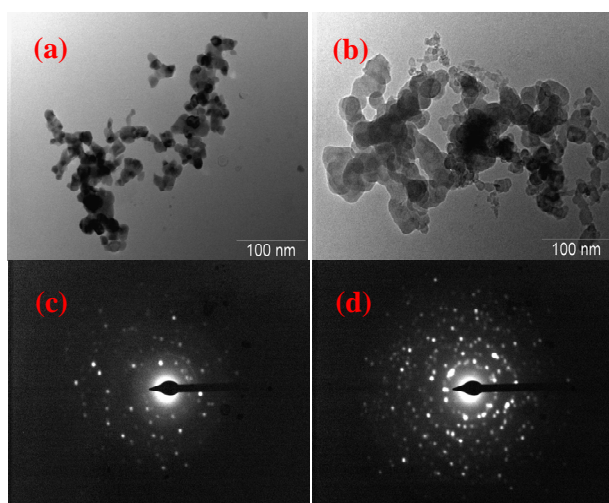

Figure 5. TEM, SAED patterns micrographs of nanocrystalline Al$_2$O$_3$ powders at different annealing condition: (a) and (c) 850 and (b) and (d) 1000˙C for 2 h.

seen that all these powders clearly appear to be in agglomerated form, which is often observed by combustion route. The selected area diffraction (SAD) pattern shown in **Figures 5(c)** and **(d)** demonstrate that the particles are crystalline in nature.

4. Conclusion

The phase transition γ- $\rightarrow$ α-Al$_2$O$_3$ occurs in three steps, as seen from X-ray diffraction (XRD), and transmission electronic microscopy (TEM) techniques. The first step, in the temperature range from 600˙C - 875˙C, constituted of γ-Al$_2$O$_3$ as seen from XRD patterns, with cubic crystal of structure. In the second step, in the temperature range from 900˙C - 1000˙C, α-Al$_2$O$_3$ as seen from XRD patterns, with corundum crystal of structure. It can also be concluded that the crystallite size calculated by XRD results is closely related to the phase transition, *i.e.*, crystallite size increases according to the phase transition variation and consequently, with the increase in temperature.

REFERENCES

[1] N. Bahlawane and T. Watanabe, "New Sol-Gel Route for the Preparation of Pure Alpha-Alumina at 950 Degrees C," *Journal of the American Ceramic Society*, Vol. 83, No. 9, 2000, pp. 2324-2326. http://dx.doi.org/10.1111/j.1151-2916.2000.tb01556.x

[2] L. A. Xue and I. W. Chen, "Influence of Additives on γ-to-α Transformation of Alumina," *Journal of Materials Science Letters*, Vol. 11, No. 8, 1992, pp. 443-445. http://dx.doi.org/10.1007/BF00731098

[3] K. Oberlander, "Applied Industrial Catalysis," Academic Press, New York, 1984, p. 63.

[4] K. Wefers, "Alumina Chemicals: Science and Technology Handbook," The American Ceramic Society, Westerville, Ohio, 1990, p. 13.

[5] H. Youn, J. W. Jang, I. Kim and K. S. J. Hong, "Low-Temperature Formation of α-Alumina by Doping of an Alumina-Sol," *Journal of Colloid and Interface Science*, Vol. 211, No. 1, 1999, pp. 110-113. http://dx.doi.org/10.1006/jcis.1998.5977

[6] H. Y. Zhu, J. D. Riches and J. C. Barry, "A-Alumina Nanofibers Prepared from Aluminum Hydrate with Poly-(ethylene oxide) Surfactant," *Chemistry of Materials*, Vol. 14, No. 5, 2002, pp. 2086-2093. http://dx.doi.org/10.1021/cm010736a

[7] S. Bhaduri, E. Zhou and S. B. Bhaduri, "Auto Ignition Processing of Nanocrystalline α-Al$_2$O$_3$," *Nanostructured Materials*, Vol. 7, No. 5, 1996, pp. 487-496. http://dx.doi.org/10.1016/0965-9773(96)00030-X

[8] S. Bhaduri, S. B. Bhaduri and E. Zhou, "Auto Ignition Synthesis and Consolidation of Al$_2$O$_3$-ZrO$_2$ Nano/Nano Composite Powders," *Journal of Materials Research*, Vol. 13, No. 1, 1998, pp. 156-165. http://dx.doi.org/10.1557/JMR.1998.0021

[9] K. C. Patil, S. T. Aruna and S. Ekambaram, "Combustion Synthesis," *Current Opinion in Solid State & Materials Science*, Vol. 2, No. 2, 1997, pp. 158-165. http://dx.doi.org/10.1016/S1359-0286(97)80060-5

[10] R. N. Das, A. Bandyopadhyay and S. Bose, "Nanocrystalline-Al$_2$O$_3$ Using Sucrose," *Journal of the American Ceramic Society*, Vol. 84, No. 10, 2001, pp. 2421-2423. http://dx.doi.org/10.1111/j.1151-2916.2001.tb01024.x

[11] A. G. Merzhanov, Z. A. Munir and J. B. Holt, "Combustion and Plasma Synthesis of High Temperature Materials," VCH, New York, 1990, p. 1.

[12] R. Garcıa, G. A. Hirata and J. McKittrick, "New Combustion Synthesis Technique for the Production of (Inx-Ga1-x)2O3 Powders: Hydrazine/Metal Nitrate Method,"

Journal of Materials Research, Vol. 16, No. 4, 2001, pp. 1059-1065. http://dx.doi.org/10.1557/JMR.2001.0147

[13] J. McKittrick, E. J. Bosze, C. F. Bacalski and L. E. Shea, "Physical Properties of Combustion Synthesized Oxide Powders ed F D S Marquis," Minerals, Metals and Materials Society, Warrendale, 1999, p. 139.

[14] B. D. Cullity, "Elements of X-Ray Diffraction," Addison-Wesley, Reading, 1967.

[15] I. Levin and D. Brandon, "Metastable Alumina Polymorphs: Crystal Structures and Transition Sequences," *Journal of the American Ceramic Society*, Vol. 81, No. 8, 1998, pp. 1995-2012. http://dx.doi.org/10.1111/j.1151-2916.1998.tb02581.x

[16] S. Roy, A. Das Sharma, S. N. Roy and H. S. Maiti, "Synthesis of Yba$_2$Cu$_3$Oδ-$_8$ Powder by Auto-Ignition of Citrate-Nitrate Gel," *Journal of Materials Research*, Vol. 8, No. 11, 1993, pp. 2761-2766. http://dx.doi.org/10.1557/JMR.1993.2761

[17] A. Chakrabort, P. S. Devi, S. Roy and H. S. Maiti, "Low-Temperature Synthesis of Ultrafine La0.84Sr0.16MnO3 Powder by an Autoignition Process," *Journal of Materials Research*, Vol. 9, No. 4, 1994, pp. 986-991. http://dx.doi.org/10.1557/JMR.1994.0986